

Experimental implementation of heat-bath algorithmic cooling using solid-state nuclear magnetic resonance

Jonathan Baugh,^{*} Osama Moussa, Colm A. Ryan, Ashwin Nayak,[†] and Raymond Laflamme[‡]
Institute for Quantum Computing, University of Waterloo, Waterloo, Ontario N2L 3G1
(Dated: Nov. 24, 2005)

The counter-intuitive properties of quantum mechanics have the potential to revolutionize information processing by enabling efficient algorithms with no known classical counterparts [1, 2]. Harnessing this power requires developing a set of building blocks [3], one of which is a method to initialize the set of quantum bits (qubits) to a known state. Additionally, fresh ancillary qubits must be available during the course of computation to achieve fault tolerance [4, 5, 6, 7]. In any physical system used to implement quantum computation, one must therefore be able to selectively and dynamically remove entropy from the part of the system that is to be mapped to qubits. One such method is an "open-system" cooling protocol in which a subset of qubits can be brought into contact with an external large heat-capacity system. Theoretical efforts [8, 9, 10] have led to an implementation-independent cooling procedure, namely heat-bath algorithmic cooling (HBAC). These efforts have culminated with the proposal of an optimal algorithm, the partner-pairing algorithm (PPA), which was used to compute the physical limits of HBAC [11]. We report here the first experimental realization of multi-step cooling of a quantum system via HBAC. The experiment was carried out using nuclear magnetic resonance (NMR) of a solid-state ensemble three-qubit system. It demonstrates the repeated repolarization of a particular qubit to an effective spin-bath temperature and alternating logical operations within the three-qubit subspace to ultimately cool a second qubit below this temperature. Demonstration of the control necessary for these operations is an important milestone in the control of solid-state NMR qubits and toward fault-tolerant quantum computing.

I. INTRODUCTION

NMR-based ensemble quantum information processing (QIP) devices have provided excellent testbeds for controlling non-trivial numbers of qubits [12, 13, 14, 15]. A solid-state NMR QIP architecture builds on this success by incorporating the essential features of the liquid-state devices while offering the potential to reach unit polarization and thus control more qubits [15, 16]. In this architecture, the abundant nuclear spins with polarization P form a large heat-capacity spin-bath that can be either coupled to, or decoupled from, a dilute, embedded ensemble of spin-labelled isotopomers that comprise the qubit register. Bulk spin-cooling procedures such as dynamic nuclear polarization are well known and capable of reaching polarizations near unity [15, 17]. This architecture is one realization within a large class of possible solid-state QIP systems in which coherently controlled qubits can be brought into contact with an external system that behaves as a heat bath. The principles and methods applied in solid-state NMR QIP will therefore apply to many other systems. An additional motivation is development of control techniques that future quantum devices will utilize. For this experiment, we develop a novel technique to implement the controlled qubit-bath interaction, and also report the first application of strongly-modulating

pulses [18] to solid-state NMR for high-fidelity, coherent qubit control.

II. THREE-QUBIT MALONIC ACID SYSTEM

The three-qubit quantum information processor used here is formed by the three spin-1/2 ^{13}C nuclei of isotopically labelled malonic acid molecules, occupying a dilute fraction of lattice sites in an otherwise unlabeled single-crystal of malonic acid (unlabeled, with the exception of naturally occurring ^{13}C isotopes at the rate of 1.1%). The concentration of labelled molecules was 3.2%. Malonic acid also contains abundant spin-1/2 ^1H nuclei, which comprise the heat-bath. Figure 1 shows the ^1H -decoupled, ^{13}C -NMR spectrum for the crystal (and crystal orientation) used in this work. The spectrum shows the NMR absorption peaks of both the qubit spins (quartets) and natural abundance ^{13}C spins (singlets), the latter being inconsequential for QIP purposes. The table in Fig. 1 lists the parameters of the ensemble qubit Hamiltonian obtained from fitting the spectrum, and also includes couplings involving the methylene protons calculated for this crystal orientation from the known crystal structure [19]. Experiments were performed at room temperature at a static magnetic field strength of 7.1 T, where the thermal ^1H polarization is $P_H \simeq 2.4 \times 10^{-5}$.

^{*}Electronic address: baugh@iqc.ca

[†]Also at Perimeter Institute for Theoretical Physics, Waterloo, ON

[‡]Electronic address: rlaflamme@iqc.ca; URL: <http://www.iqc.ca>;
Also at Perimeter Institute for Theoretical Physics, Waterloo, ON

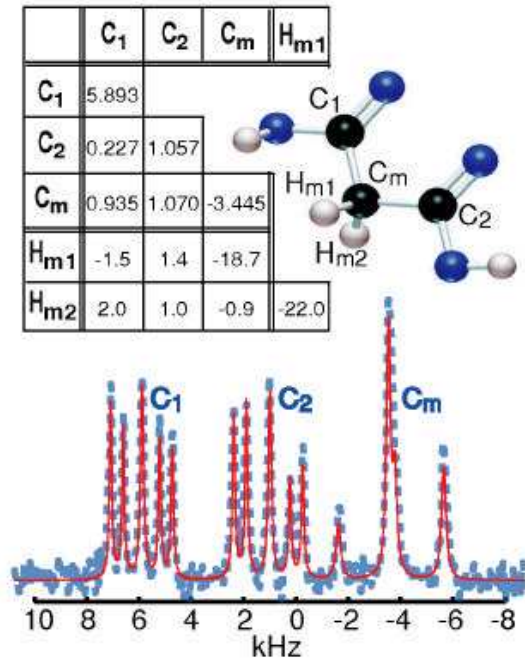


FIG. 1: Characteristics of the dilute $3\text{-}^{13}\text{C}$ malonic acid spin system. (below) ^1H -decoupled, ^{13}C spectrum near the $[010]$ orientation with respect to the static magnetic field. The blue-dashed line is the experimental NMR absorption spectrum, and the solid-red line is a fit. Multiplet assignments are indicated by the labels C_1 , C_2 and C_m . The central peaks in each multiplet correspond to natural abundance ^{13}C in the sample, which are inconsequential for QIP purposes. The peak height differences in the $3\text{-}^{13}\text{C}$ molecule peaks indicate the strong coupling regime, i.e. the $^{13}\text{C}\text{-}^{13}\text{C}$ intramolecular dipolar couplings are significant compared to the relative chemical shifts. (above) Table showing the ^{13}C rotating-frame Hamiltonian parameters (chemical shifts along diagonal; dipolar coupling strengths off-diagonal; all values in kHz) obtained from the spectral fit. It also includes calculated dipolar couplings involving the methylene protons based on the atomic coordinates [19] and the crystal orientation obtained from the spectral fit.

III. REFRESH OPERATION

In this orientation, the methylene carbon C_m has a dipolar coupling of 19 kHz to H_{m1} of the methylene ^1H pair, whereas no other $^{13}\text{C}\text{-}^1\text{H}$ dipolar coupling in the system is larger than 2 kHz. Therefore, a spin-exchange Hamiltonian of the form

$$\mathcal{H}_{ex} = \sum_{j \in C, k \in H} \frac{D_{jk}}{3} \frac{\sigma_z^j \sigma_z^k + \sigma_y^j \sigma_y^k + \sigma_x^j \sigma_x^k}{2} \quad (1)$$

that couples the two nuclear species will generate dynamics dominated by the large $C_m\text{-}H_{m1}$ coupling at short times (the D_{jk} are $^{13}\text{C}\text{-}^1\text{H}$ dipolar couplings, indices run

over $^{13}\text{C}, ^1\text{H}$ nuclei, respectively, and σ_β^α is the β -axis Pauli operator for spin α). Starting from the natural coupling Hamiltonian,

$$\mathcal{H}_{nat} = \sum_{j \in C, k \in H} D_{jk} \sigma_z^j \sigma_z^k / 2, \quad (2)$$

we applied a multiple-pulse 'time-suspension' sequence [20] synchronously to both ^{13}C and ^1H spins to create the effective spin-exchange Hamiltonian (in the toggling frame), to lowest order in the Magnus expansion of the average Hamiltonian [21]. Application of the sequence for the $C_m\text{-}H_{m1}$ exchange period $\tau = \frac{3}{4 \times 19 \text{kHz}} \simeq 40 \mu\text{s}$ results in an approximate swap gate (state exchange) between the C_m and H_{m1} spins. With an initial bulk ^1H polarization P_H , this procedure yields a selective dynamic transfer of polarization $P' = \eta P_H$ to C_m , where $0 \leq \eta \leq 1$ and ideally $|\eta| = 1$. We define the effective spin-bath temperature to be that which corresponds to the experimentally obtained P' under this procedure, and refer to this transfer as a refresh operation. We obtained $P' \simeq 0.83 P_H$ experimentally, and found that repeated refresh operations showed no loss in efficiency given at least a 6 ms delay for $^1\text{H}\text{-}^1\text{H}$ equilibration. However, we observed a decay of P_H as a function of the number of repetitions, due to accumulated control errors, which lead to an identical loss in the refresh polarization.

IV. IMPLEMENTATION OF PARTNER-PAIRING ALGORITHM

The experiment consists of the first six operations of the partner-pairing algorithm (PPA) on three qubits: three refresh operations, and three permutation gates that operate on the qubit register. This is described in the quantum circuit diagram of Fig. 2. During the register operations, the ^1H polarization is first rotated into the transverse plane, and then 'spin-locked' by a strong, phase-matched RF field that both preserves the bulk ^1H polarization and decouples the $^1\text{H}\text{-}^{13}\text{C}$ dipolar interactions. Since $^1\text{H}\text{-}^1\text{H}$ dipolar interactions are merely scaled by a factor $-1/2$ under spin-locking, H_{m1} is allowed to equilibrate with the bulk ^1H nuclei via spin diffusion. This occurs on a timescale longer than the transverse dephasing time ($T_2(H_m) \sim 100 \mu\text{s}$), but much shorter than the spin-lattice relaxation time ($T_1^H \sim 50\text{s}$) of H_{m1} . Hence, H_{m1} plays the role of the fast-relaxing qubit described in the protocol of Schulman et al. [11]. The first two register operations are swap gates; the third is a three-bit compression (3BC) gate [8, 9, 10] that boosts the polarization of the first qubit, C_1 , at the expense of the polarizations of the other two qubits. Ideally, the protocol builds a uniform polarization on all three qubits corresponding to the bath polarization (first five steps), then selectively transfers as much entropy as possible from the first qubit to the other two (last step).

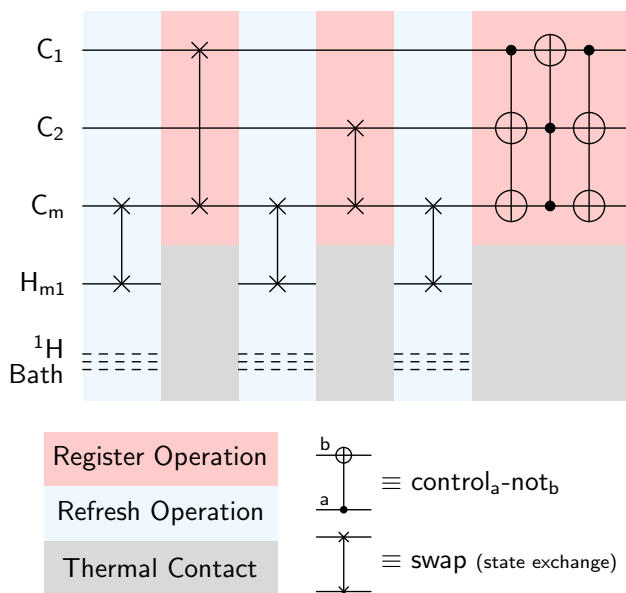


FIG. 2: Schematic quantum circuit diagram of the implemented protocol. Time flows from left to right. The three-bit compression (3BC) gate is shown here decomposed as control-not gates and a control-control-not (Toffoli) gate. The gate sequence corresponds to the first six steps of the partner-pairing algorithm [11] on three qubits. The input state is a collective polarization of the bulk ^1H spins. The refresh operation is approximately $40\mu\text{s}$ in duration, whereas the register operations are between 0.7 and 1.3 ms in duration. Thermal contact takes place during ^1H spin-locking pulses that begin just prior to the register operations, and extend an additional 12 ms after each operation. H_{m1} can be thought of as an additional ‘special purpose’ qubit in this experiment; despite non-selective ^1H control (due to bulk hydrogenation), the refresh and thermal contact operations could be performed using collective ^1H control. Thus, H_{m1} serves as a fast-relaxing ‘qubit’ and the bulk ^1H -bath as a large heat-capacity thermal bath.

The last step (3BC) leads to a polarization boost by a factor of $3/2$ on the first qubit. Subsequently, the heated qubits can be re-cooled to the spin-bath temperature, and the compression step repeated, iteratively, until the asymptotic value of the first-bit polarization is reached. This limiting polarization depends only on the number of qubits and the bath polarization [11], and is ideally $P(C_1) = 2P'$ for three qubits (for n qubits it is $2^{n-2}P'$ in the regime $P' \ll 2^{-n}$, and 1.0 in the regime $P' \gg 2^{-n}$ (refs. [11, 22]). The first six steps carried out here should yield a polarization of $1.5P'$ on C_1 , assuming ideal operations.

The control operations performed herein are quantum control operations: state-independent unitary rotations in the Hilbert space. However, it should be noted that the HBAC gates are all permutations that map computational basis states to other computational basis states. Therefore, gate fidelities were measured with respect to correlation with these known states,

rather than the manifold of generic quantum states. We took advantage of this property to further optimize the control parameters of the ^{13}C gates (register operations) for the state-specific transformations of the protocol. These operations were carried out using numerically optimized control sequences referred to as strongly-modulating pulses [18]. Such pulses drive the system strongly at all times, such that the average RF amplitude is comparable to, or greater than, the magnitude of the internal Hamiltonian. This allows inhomogeneities in the ensemble qubit Hamiltonian to be efficiently refocused, so that ensemble coherence is better maintained throughout the gate operations.

In this set of experiments, the ^{13}C qubit spins are initialized to infinite temperature (a preceding broadband ^{13}C $\pi/2$ excitation pulse is followed by a dephasing period in which ^1H dipolar fields effectively dephase the ^{13}C polarization). Following the fifth step, polarizations (in units of P') of 0.88, 0.83 and 0.76 (± 0.03) are built up on C_1 , C_2 and C_m , respectively. The final 3BC operation yields $P(C_1)/P' = 1.22 \pm 0.03$, a boost of 48% compared to the average polarization (0.82) following step five. Despite control imperfections that effectively heat the qubits at each step, we are able to cool the C_1 qubit ensemble well below the effective ^1H spin-bath temperature.

V. RESULTS

The results are summarized in Fig. 3; in (a) are shown the spectral intensities corresponding to ^{13}C spin polarizations following each of the six steps, and in (b) the integrated intensities are graphed in comparison with the ideal values. We note that the overall fidelity of the experiment, $F = 1.22/1.50 = 0.81$, implies an error per step of 3.7%. This error rate is only about a factor of two larger than the average error per two-qubit gate obtained in a benchmark liquid-state NMR QIP experiment [12]. Furthermore, the state-correlation fidelity of the 3BC gate over the polarizations on all three qubits is 0.96 ± 0.03 . From Fig. 3(b), it can be seen that the fidelity of the refresh operation drops off roughly quadratically in the number of steps; this is consistent with the loss of bulk ^1H polarization due to pulse imperfections both in the multiple-pulse refresh operations and in the spin-locking sequence. Since the broadband pulses have been optimized for flip-angle in these sequences, we suspect that the remaining errors are mainly due to switching transients that occur in the tuned RF circuitry of the NMR probehead, and to a lesser extent off-resonance and finite pulse-width effects that modify the average Hamiltonian [20]. Similar effects lead to imperfect fidelity of the ^{13}C control. With suitable improvements to the resonant circuit response and by incorporating numerical optimization of the multiple-pulse refresh operations, we expect

that several iterations of the protocol could be carried out and that the limiting polarization of $2P'$ could be approached in this system. The same methodologies should also be applicable in larger qubit systems with similar architecture. For a 6-qubit system using the PPA, a bath polarization $P > 0.2$ would be sufficient, in principle, to reach a pure state on one qubit [22]. Such bulk nuclear polarizations are well within reach via well-known dynamic nuclear polarization techniques [17]; for example, unpaired electron spins at defects ($g = 2$) in a field of 3.4 T and at temperature 4.2 K are polarized to 0.5.

This work demonstrates that solid-state NMR QIP devices could be used to implement active error correction. Given a bath polarization near unity, the refresh operation implemented here would constitute the dynamic resetting of a chosen qubit. This would allow a new NMR-based testbed for the ideas of quantum error correction and for controlled open-system quantum dynamics in the regime of high state purity and up to ~ 20 qubits.

VI. METHODS

NMR experiments were carried out at room temperature on a Bruker Avance solid-state spectrometer operating at a field of 7.1 T, and home-built dual channel RF probe. The sample coil had an inner diameter of 3 mm, and the employed $\pi/2$ broadband pulse lengths were $1.25\mu\text{s}$ and $0.75\mu\text{s}$ for ^{13}C and ^1H , respectively. The sample was a $4.5 \times 1 \times 1 \text{ mm}^3$ single crystal of malonic acid grown from aqueous solution with a 3.2% molecular fraction of 3- ^{13}C labelled molecules. Spectra were obtained by signal averaging for 80 scans. The proton spin-lattice relaxation time was $T_1^H = 50\text{s}$, so the delay between scans was set to $6T_1^H = 300\text{s}$. Design of the strongly-modulating ^{13}C pulses followed very closely the methodology described in ref. [18], and penalty functions were adjusted to favor average RF amplitudes comparable to or greater than the magnitude of the ^{13}C rotating-frame Hamiltonian. These pulses were optimized and simulated over a 5-point distribution of RF amplitude corresponding to the measured distribution over the spin ensemble ($\sigma = 6.2\%$ in RF amplitude). The 'time-suspension' sequence applied synchronously to ^{13}C and ^1H was a 12-pulse subsequence of the Cory 48-pulse sequence [20]. The delays between pulses were adjusted so that the total length of the sequence was $40\mu\text{s}$. ^1H spin-locking/decoupling was carried out at RF amplitude of

250 kHz. The spectra in Fig. 3 were obtained by applying a $\pi/2$ broadband pulse to read out the spin polarizations. The readout pulses were preceded by a 1.5 ms delay in which ^1H decoupling was on but any off-diagonal terms in the ^{13}C spin density matrix would significantly dephase ($T_2^* \simeq 2\text{ms}$). The absolute value of the refresh polarization P' was determined by comparing the initial refresh

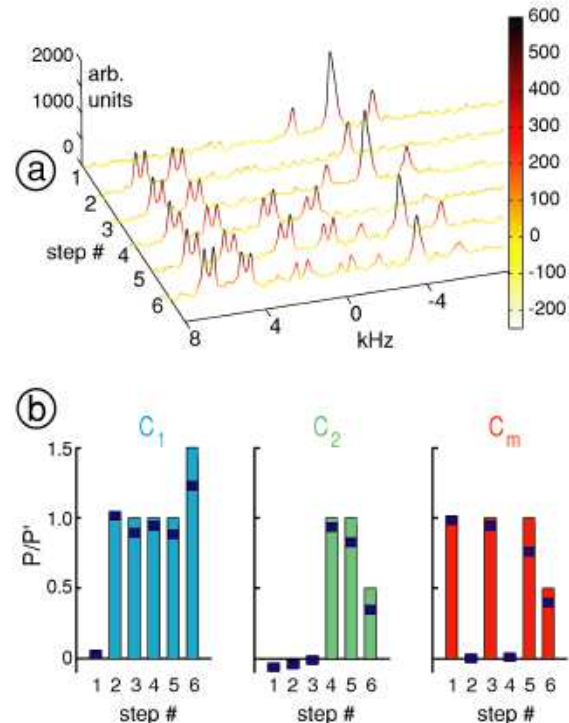


FIG. 3: Experimental results in terms of ^{13}C spectra and their integrated intensities. (a) Readout spectra obtained following each of the six steps in the protocol. The integrated peak intensities for each multiplet correspond to the ensemble spin polarizations. The natural abundance C_m signal that appears at each refresh step (adding to the intensity of the central peaks) should be ignored; we are only interested in the part of the signal arising from the 3- ^{13}C qubit molecules, which can be seen clearly in the C_1 and C_2 spectral regions. (b) Bars indicate ideal qubit polarizations at each step; experimental values obtained from integration of the above spectra are shown as shaded bands, whose thickness indicates experimental uncertainty.

polarization on C_m and the thermal equilibrium ^{13}C polarization P_C measured in a separate experiment. These yield the ratio of P' to P_C , and P' to P_H using the fact that $P_H = 3.98P_C$.

[1] M. A. Nielsen and I. L. Chuang, *Quantum Computation and Quantum Information* (Cambridge University Press, Cambridge, UK, 2000).

[2] Quant. Inform. Process. **3**, 1 (2004), special issue.

[3] D. P. DiVincenzo, Fort. der Phys. **48**, 771 (2000), quant-ph/0002077.

- [4] E. Knill, R. Laflamme, and W. H. Zurek, *Science* **279**, 342 (1998).
- [5] A. Y. Kitaev, in *Quantum Communication, Computing and Measurement* (Plenum, New York, USA, 1997), pp. 181–188.
- [6] D. Aharonov and M. Ben-Or, in *Proc. 29th. Ann. ACM Symp. on Theory of Computing* (1997), longer version quant-ph/9906129, quant-ph/9611025.
- [7] J. Preskill, *Proc. R. Soc. Lond. A* **454**, 385 (1998), quant-ph/9705031.
- [8] L. Schulman and U. Vazirani, *Proc. of the 31th Annual ACM Symposium on Theory of Computing* pp. 322–329 (1999).
- [9] P. O. Boykin, T. Mor, V. Roychowdhury, F. Vatan, and R. Vrijen, *Proc. Natl. Acad. Sci. USA* **99**, 3388 (2002), quant-ph/0106093.
- [10] J. M. Fernandez, S. Lloyd, T. Mor, and V. Roychowdhury, *Int. J. Quant. Inform.* **2**, 461 (2004).
- [11] L. Schulman, T. Mor, and Y. Weinstein, *Phys. Rev. Lett.* **94**, 120501 (2005).
- [12] E. Knill, R. Laflamme, R. Martinez, and C.-H. Tseng, *Nature* **404**, 368 (2000), quant-ph/9908051, URL <http://www.ariv.org/abs/quant-ph/9908051>.
- [13] N. Gershenfeld and I. L. Chuang, **275**, 350 (1997).
- [14] D. G. Cory, M. D. Price, and T. F. Havel, *Physica D* **120**, 82 (1998), quant-ph/9709001.
- [15] D. G. Cory, R. Laflamme, E. Knill, L. Viola, T. F. Havel, N. Boulant, G. Boutis, E. Fortunato, S. Lloyd, R. Martinez, et al., *Fort. der Phys. special issue, Experimental Proposals for Quantum Computation* **48** (2000), quant-ph/0004104.
- [16] G. M. Leskowitz, R. A. Olsen, N. Ghaderi, and L. J. Mueller, *J. Chem. Phys.* **119**, 1643 (2003).
- [17] A. Abragam and M. Goldman, *Nuclear Magnetism: Order and Disorder* (Oxford University Press, Oxford, England, 1982).
- [18] E. M. Fortunato, M. A. Pravia, N. Boulant, G. Teklemariam, T. F. Havel, and D. G. Cory, *J. Chem. Phys.* **116**, 7599 (2002).
- [19] N. R. Jagannathan, S. S. Rajan, and E. Subramanian, *J. Chem. Cryst.* **24**, 75 (1994).
- [20] D. G. Cory, J. B. Miller, and A. N. Garroway, *J. Mag. Res.* **90**, 205 (1990).
- [21] U. Haeberlen, *High Resolution NMR in Solids: Selective Averaging* (Academic Press, New York, USA, 1976).
- [22] O. Moussa, *On heat-bath algorithmic cooling and its implementation in solid-state NMR* (2005), MSc. thesis, <http://www.iqc.ca/omoussa/work/thesis>.

We gratefully acknowledge: D. G. Cory, T. F. Havel, and C. Ramanathan for discussions and use of NMR simulation code; W. P. Power, M. Ditty and N. J. Taylor for facility use and experimental assistance; ARDA and NSERC for support. O. M. acknowledges the Ontario Ministry of Training, Colleges and Universities for support. Correspondence and requests for material should be sent to J. B. (e-mail: baugh@iqc.ca).